DOPPLER-BASED DOA ESTIMATION WITH AN ESPAR ANTENNA OPERATED ON CYCLICALLY CONTROLLED REACTANCES

Tomoshige FURUHI†, Osamu SHIBATA†,
Akifumi HIRATA‡, Makoto TAROMARU‡ and Takashi OHIRA‡
†Murata Manufacturing Co., Ltd.
1-10-1 Higashikotari, Nagaokakyo, Kyoto 617-8555, Japan
‡ATR Wave Engineering Laboratories
2-2-2 Hikaridai, Keihanna Science City, Kyoto 619-0288, Japan
E-mail: furuhi@murata.co.jp

1. Introduction

The Electronically Steerable Parasitic Array Radiator (ESPAR) antenna [1] is a promising device for controlling the beam direction with simple structure and low power. Several algorithms using ESPAR antenna have been proposed for estimating direction of arrival (DOA). For example, Plapous et al. [2] proposed reactance-domain MUSIC algorithm which can estimate DOA with high resolution based on output signals obtained from several reactance sets. Taillefer et al. [3] proposed another algorithm which can estimate DOA by using power output cross-correlation and antenna pattern diversity.

Doppler direction finder (DDF) [4] is also an useful method for DOA estimation. DDF has an electronically switched circular-array antenna, which generates quasi-Doppler frequency shift. The phase difference between the Doppler frequency shift of received signal and periodical antenna-switching signal provides the DOA of the received signal.

Since ESPAR antenna is different from DDF's antenna in the viewpoint that the signal directly received by the center element is inevitably added to the output-port signal, it cannot be applied directly to DDF. However, accurate estimation is realized by applying two means: (a) adding Band Elimination Filter (BEF), and (b) optimizing the distance between the center element and the parasitic ones.

In this paper, a novel method for DOA estimation is proposed which utilizes quasi-Doppler frequency shift raised by electronically controlled parasitic elements of ESPAR antenna. The method has several advantages as compared with conventional DDF in terms of simple configuration, small size, low consumption power and operating without transmission cables.

2. Configuration

Figure 1 shows the block diagram of the proposed configuration with 13-element ESPAR antenna. The ESPAR antenna consists of one center element connected to an output-port and 12 parasitic ones on the ground plane. The parasitic elements are arranged circularly with the distance of r=0.383λ_c from the center element, where λ_c is the wavelength of the incident wave. Each parasitic element is connected to variable impedance circuit, which is controlled by the impedance controller. The impedance of each circuit is varied cyclically with period T_r as shown in Fig. 2. It is assumed that only the parasitic element connected to low ("L") impedance has mutual coupling with the center element. Thus, the coupled parasitic element operates as if it is cyclically hopping around the center element, and generates quasi-Doppler frequency shift.

The Band Pass Filter (BPF) and the BEF are connected to the output-port of ESPAR antenna in order to suppress higher harmonics generated by cyclical antenna switching and the incident wave frequency (ω_c=2$\pi c/\lambda_c$), respectively. The filtered output produces almost sinusoidal frequency change. The inserted BEF does not distort the output signal by designing the value of r properly. Frequency discriminator converts the frequency change to voltage. The estimated DOA is calculated from the output signal of the phase comparator which measures the phase difference between the output of the frequency discriminator and that of the timing signal generator.

3. Principles of DOA Estimation

The output of ESPAR antenna is expressed as a linear combination of excited voltages of respective antenna elements [1]. In the proposed method, since the values of variable impedance circuits are cyclically controlled as described above, the antenna output is expressed as:

$$y(t) = a_c y_c(t) + a_r y_r(t) \quad (1)$$

ISBN: 89-86522-77-2 94460©KEES

where a_c and a_r are constants, $y_c(t)$ is the amplitude of incident wave at the position of center element and $y_r(t)$ is that at the cyclically hopping position of coupled parasitic element. It should be noted that $y_c(t)$ and $y_r(t)$ are defined as to neglect mutual couplings among the antenna elements. Since $y_c(t)$ has only frequency component ω_c and the BEF is designed to reject it, the filtered output signal, $\hat{y}(t)$, is expressed as:

$$\hat{y}(t) = a_r \hat{y}_r(t) \tag{2}$$

where $\hat{y}_r(t)$ is the filtered output of $y_r(t)$. Thus, it is enough to get the incident-wave signal received at the cyclically hopping position of coupled parasitic element for obtaining $\hat{y}(t)$.

As shown in Fig. 3, $\vec{R}(t)$ is defined as the position of coupled parasitic element at time t:

$$\vec{R}(t) = \left(-r\cos\frac{2\pi}{n}\left\langle \frac{n}{T_r}t \right\rangle, \quad -r\sin\frac{2\pi}{n}\left\langle \frac{n}{T_r}t \right\rangle \right) \tag{3}$$

where n is the number of parasitic elements, $\langle x \rangle$ denotes the integer nearest to x. Defining the azimuth angle of the incident wave to be α (see Fig. 3), the phase of incident wave at the position of coupled parasitic element at time t is expressed as:

$$\phi(t) = -\frac{2\pi}{\lambda_c}\vec{R}(t)\cdot(-\cos\alpha, \quad -\sin\alpha)^T = -\frac{2\pi r}{\lambda_c}\cos\left(\frac{2\pi}{n}\left\langle \frac{n}{T_r}t \right\rangle - \alpha\right) \tag{4}$$

where T is the matrix transpose operator. Since $y_r(t)$ is expressed as $y_r(t) = b\sin(\omega_c t + \phi(t))$, where b is a constant, it is written from Eq. (4) as:

$$y_r(t) = b\sin\left[\omega_c t - \frac{2\pi r}{\lambda_c}\cos\left(\frac{2\pi}{n}\left\langle \frac{n}{T_r}t \right\rangle - \alpha\right)\right]. \tag{5}$$

By expanding $\langle (n/T_r)t \rangle$, Eq. (5) is rewritten as:

$$y_r(t) = b\left\{\sin\left[\omega_c t - \frac{2\pi r}{\lambda_c}\cos\left(\frac{2\pi}{T_r}t - \alpha\right)\right]\cdot\sum_{k=-\infty}^{\infty}\delta\left(t - k\frac{T_r}{n}\right)\right\}\otimes u\left(\frac{n}{T_r}t\right) = b\left\{\sin\psi(t)\cdot\sum_{k=-\infty}^{\infty}\delta\left(t - k\frac{T_r}{n}\right)\right\}\otimes u\left(\frac{n}{T_r}t\right) \tag{6}$$

where $\delta(x)$ is delta function, $\otimes$ denotes convolution operator,

$$u(\tau) \overset{\text{def}}{\equiv} \begin{cases} 1 & \text{for } |\tau| < \dfrac{1}{2} \\ 0 & \text{otherwise} \end{cases} \tag{7}$$

and

$$\psi(t) \overset{\text{def}}{\equiv} \omega_c t - \frac{2\pi r}{\lambda_c}\cos\left(\frac{2\pi}{T_r}t - \alpha\right). \tag{8}$$

As a simple case, when the number of parasitic elements, n, is large enough, Eq. (6) approaches $b\sin\psi(t)$. Defining $\tilde{\omega}(t)$ as the instantaneous frequency of $b\sin\psi(t)$, it is expressed as:

$$\tilde{\omega}(t) = \frac{d\psi(t)}{dt} = \omega_c + \frac{2\pi r}{\lambda_c}\frac{2\pi}{T_r}\sin\left(\frac{2\pi}{T_r}t - \alpha\right). \tag{9}$$

Equation (9) shows that temporal variation of $\tilde{\omega}$ is sinusoidal and that the phase of its frequency change depends upon the incident azimuth angle α. Therefore, DOA is easily estimated based on $\tilde{\omega}(t)$ for enough large n. From Eq. (8), $b\sin\psi(t)$ is a frequency-modulated signal, which means that (a) its frequency spectrum discontinuously spreads to $\omega_c \pm p\omega_r$, where p is an integer and $\omega_r = 2\pi/T_r$, and (b) the amplitudes of the incident-wave frequency ω_c (p=0) and that of p-th sideband ($p \neq 0$) are proportional to $J_p(m_f)$, where $J_p(x)$ is the p-th order Bessel function of the first kind, and m_f is the modulation index. From Eq. (8), m_f is expressed as:

$$m_f = 2\pi r/\lambda_c. \tag{10}$$

Since the value of r ($=0.383\lambda_c$) is determined to satisfy $J_0(m_f) = J_0(2.405) \cong 0$, the frequency component ω_c in $y_r(t)$ is eliminated. Therefore, frequency spectrum of $\hat{y}_r(t)$ is not distorted with the insertion of BEF.

When n is not large enough, the difference between $y_r(t)$ and $b\sin\psi(t)$ has to be considered. The Fourier transform of Eq. (6) is derived as follows:

$$\Im(y_r) = b\left\{\Im(\sin\psi(t))\otimes\Im\left(\sum_{k=-\infty}^{\infty}\delta\left(t - k\frac{T_r}{n}\right)\right)\right\}\cdot\Im\left(u\left(\frac{n}{T_r}t\right)\right) = b'\left\{\Im(\sin\psi(t))\otimes\sum_{k=-\infty}^{\infty}\delta(\omega - kn\omega_r)\right\}\cdot U\left(\frac{2\pi\omega}{n\omega_r}\right) \tag{11}$$

where b' is a constant, $\Im$ denotes Fourier transform operator, and $U(\Omega)$ is defined as:

$$U(\Omega) \equiv \Im(u(\tau)) = (2/\Omega)\sin(\Omega/2) = \mathrm{sinc}(\Omega/2). \tag{12}$$

Figure 4 shows the frequency spectrum of $y_r(t)$ calculated from Eq. (11) for n=12. Although

"image spectrum" is brought at both sides of "fundamental spectrum" ($\Im(\sin\psi(t))$) as a result of convolution with $\delta(\omega-kn\omega_r)$ in Eq. (11), the separation between "fundamental" and "image" is so wide that it is possible to suppress "image" by adding BPF. Thus, the filtered output is similar to that in case of $n \to \infty$. The calculated results of phase shift of Eq. (6) and the BPF output are shown in Fig. 5. It shows that the BPF smoothes the discontinuous variation of phase shift to sinusoidal. As a result, the frequency shift also becomes sinusoidal. Therefore, accurate estimation of DOA is realized based on the phase of frequency shift of $\hat{y}_r(t)$.

The width of separation between "fundamental" and "image" in Fig. 4 is determined by $n\omega_r$. Smaller n gives narrow separation which deteriorates estimation accuracy.

4. Simulations

The DOA estimation error is simulated for three cases: one incident wave, one incident wave with white noise, and two coherent incident waves. The estimated DOA is calculated based on the time when instantaneous frequency of the simulated filtered output reaches maximal value.

4.1. One incident wave

The simulation parameters for one incident wave are shown in Table 1. Dependence of estimation error on n is shown in Fig. 6. The estimation error decreases remarkably with increasing n and high accuracy with estimation error as small as 0.0012 degree is expected for n=12.

4.2. One incident wave with white noise

Estimation error for one incident wave with white noise is calculated for n=12 and α=0 degree. The power of noise is assumed to be white noise in the pass band of BPF. The estimation error averaged over 100 trials is shown in Fig. 7, which shows that the standard deviation of estimation error decreases in proportion to $(S/N)^{-1/2}$.

4.3. Two coherent incident waves with different power

Estimation error for two coherent incident waves is calculated for n=12. The incident azimuth angle for the higher-power wave α is assumed to be 0 degree, while that for the lower-power wave is varied from 0 to 180 degrees. Dependence of estimation error for the higher-power wave on power ratio is shown in Fig. 8. It is found that the estimation error is inversely proportional to the square root of the power ratio.

5. Conclusion

A novel method of DOA estimation is proposed and simulation results are shown. The method utilizes quasi-Doppler frequency shift raised by electronically controlled parasitic elements of ESPAR antenna. The key parameters for accurate estimation are found to be the array radius of parasitic elements, the number of those, and the properties of filters. The simulated results for configuration with 13-element ESPAR antenna show that accurate DOA with estimation error less than 0.002 degree is expected. The proposed method seems to be useful for accurate DOA estimation with simple configuration, small size, and low power consumption.

References

[1] T. Ohira and J. Cheng, "Analog Smart Antennas," in Adaptive Antenna Arrays, ed. S. Chandran, pp. 184-204, Springer Verlag, Berlin, June 2003.

[2] C. Plapous, J. Cheng, E. Taillefer, A. Hirata, and T. Ohira, "Reactance Domain MUSIC Algorithm for Electronically Steerable Parasitic Radiator," IEEE Trans. Antennas Propagation, AP-52, 12, pp. 3257-3264, Dec. 2004.

[3] E. Taillefer, A. Hirata, and T. Ohira, "Direction-of-arrival estimation using radiation power pattern with an Espar antenna," IEEE Trans. Antennas Propagation, AP-53, 2, pp.678-684, Feb. 2005.

[4] H. D. Kennedy and W. Wharton, "Direction-Finding Antennas and Systems," in Antenna Engineering Handbook 2nd edition, ed. R. C. Johnson and H. Jasik, pp. 39.21-39.22, McGraw-Hill, New York, 1961.

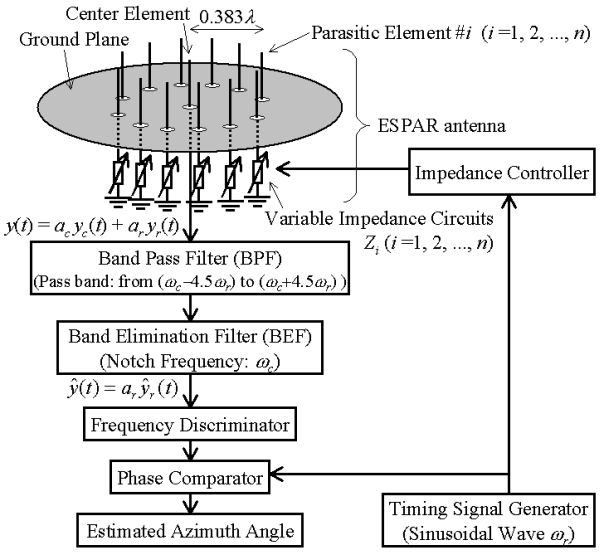

Fig. 1 Proposed Configuration with 13-element ESPAR antenna

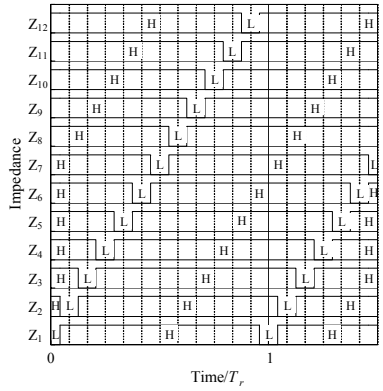

Fig. 2 Variation of impedance Z_i
('H': high impedance, 'L': low impedance)

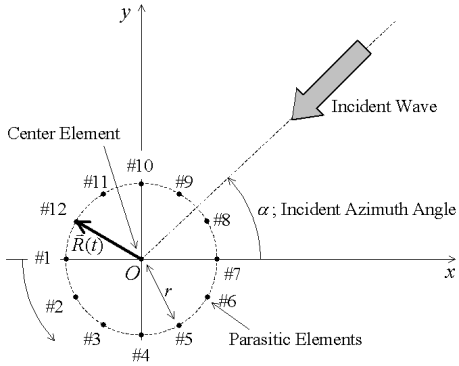

Fig. 3 Arrangement of ESPAR antenna and incident wave

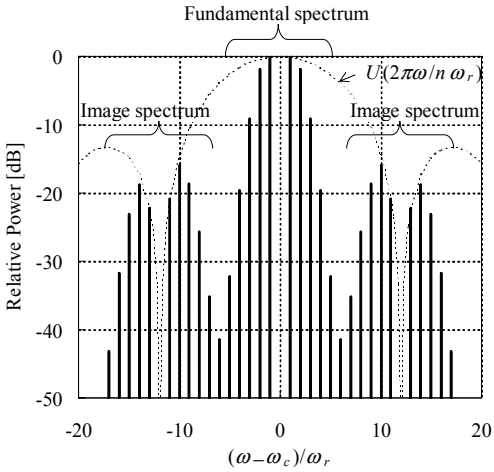

Fig. 4 Frequency spectrum of the antenna output for n=12

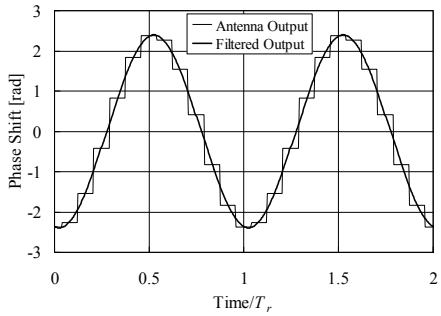

Fig. 5 Phase shift of antenna output and that of filtered output (incident azimuth angle α=10 degrees)

Table 1 Simulation parameters for one incident wave

Incident wave	Number of incident wave: 1 Incident azimuth angle: α=0, 1, 2, …, 180 degrees Frequency: $\omega_c/2\pi$=5.2GHz
Noise	none
Number of parasitic elements	n=6, 8, 12
Pass band of BPF	For n=6 or 8, from $(\omega_c-2.5\omega_r)$ to $(\omega_c+2.5\omega_r)$. For n=12, from $(\omega_c-4.5\omega_r)$ to $(\omega_c+4.5\omega_r)$.
Switching period of the coupled parasitic element	T_r=1.2μs ($\omega_r/2\pi$=(1/1.2)MHz)

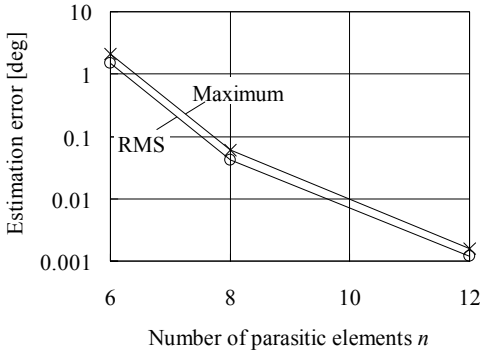

Fig. 6 Estimation error for one incident wave

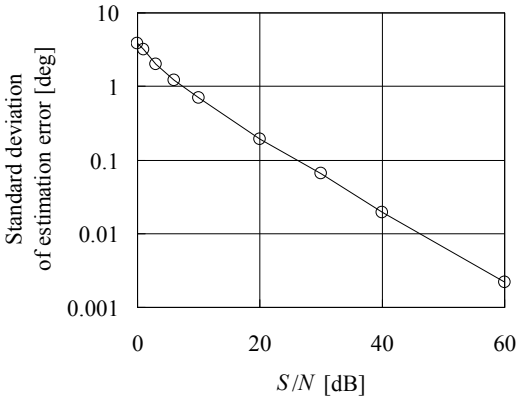

Fig. 7 Estimation error averaged over 100 trials for one incident wave with white noise for n=12

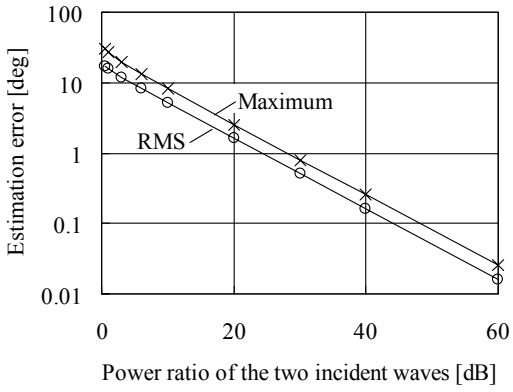

Fig. 8 Estimation error for two coherent incident waves for n=12